

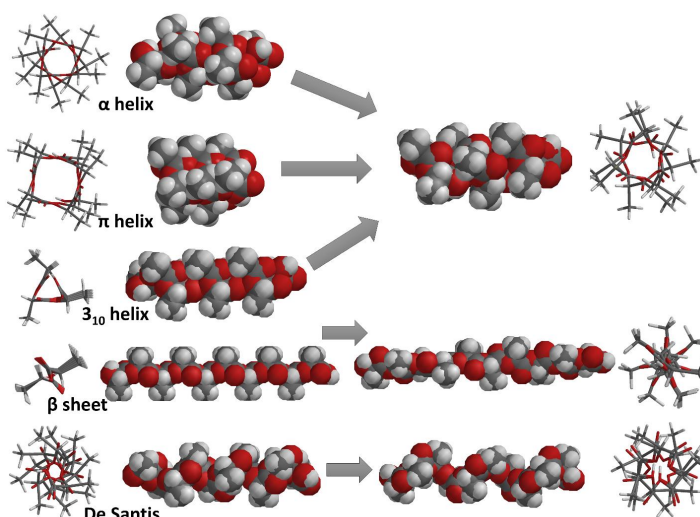
A CRITICAL REVIEW OF COMPUTATIONAL EFFORTS TOWARDS IDENTIFYING SECONDARY STRUCTURE ELEMENTS IN POLYLACTIC ACID (PLA)

Izabella IRSAI, Szilárd PESEK and Radu SILAGHI-DUMITRESCU*

Department of Chemistry, Babeş-Bolyai University, 11 Arany Janos str, Cluj-Napoca 400028, Roumania

Received April 5, 2023

Poly(lactic acid) (PLA) may be regarded as an analogue of a poly-alanine oligo/polypeptide, where the amino group has been replaced by a hydroxyl. As a consequence, a series of studies have explored the possibility that PLA can adopt peptide-type secondary structures – *i.e.*, repetitive structural patterns characterized by intramolecular hydrogen bonds between neighboring functional groups. To this end, computational techniques (molecular mechanics, semiempirical, Hartree-Fock, density functional theory (DFT) geometry optimizations of isolated oligomers of lactic acid (generally ten-unit oligomers), or oligomers attached to solid surfaces, or dimers have been reported, as well as spectral simulations thereof – looking at relative stabilities of helices (α , π , 3_{10}), and β sheets. A significant variation in the predicted structures and spectra was noted, depending on the computational method employed. With the most accurate method available (a DFT functional parametrized especially for describing non-covalent interactions), in isolated PLA models the π helix was found to be the most likely structure, closely followed by the 3_{10} helix, and β sheets being the least stable. We review here these data and add two important elements: (1) first, a comparison with an experimentally-derived model of PLA, proposed by De Santis, and (2) second, a Ramachandran analysis of the Φ and Ψ angles in the optimized geometries. It is shown that (1) the De Santis structure is in fact slightly more stable than the helices, and (2) the optimized geometries in fact stray far from the initial Φ , Ψ values – to the extent that all of the peptide-like secondary structures in fact end up as turns (mostly type III β turns), while the DFT-optimized De Santis structure has no classical correspondent in the Ramachandran series of secondary structures.



INTRODUCTION

Lactic acid (LA) plays a vital role in the glycolytic energy cycle of organisms, in

maintaining the growth and development of living organisms.¹ Poly(lactic acid) (PLA) is produced from renewable resources, for example corn or straw, the great advantage being that it is

* Corresponding author: radu.silaghi@ubbcluj.ro

completely biodegradable.^{2,3} Thus it is environmentally friendly and decomposes into water and carbon dioxide thanks to microbes. This gives it the status of one of the most important biodegradable polymeric material on the market.^{4,5} The PLA monomer, lactic acid, is easily obtained in nature, it is obtained by fermenting sugars and converting the monomers by hydrolysis.⁶ PLA has good thermoplasticity, so it can also be used for the preparation or processing of plastic materials, thus obtaining films and fibers.^{7,8} PLA is not affected by swelling or solvent dissolution during industrial processing, and the processing temperature is around 170–230°C, which makes it suitable for processing methods such as extrusion, biaxial stretching or spinning.^{9–11} PLA has good biocompatibility, biodegradability, antibacterial and flame retardant properties, and is water and oil resistant. It can be used in the clothing industry, medical production, packaging materials.^{12–16}

LA is a chiral molecule with d- and l-type isomers, thus forming three forms of PLA: poly-l-lactic acid (PLLA), poly-d-lactic acid (PDLA) and poly-D,L-lactic acid (PDLLA).¹⁷ Regarding the optical activity, we define two compositions – L and D enantiomers – so that polylactic acid can be crystallized in three forms (α , β and γ).^{18–20} PLA began to be used in surgical sutures and bone implants in the 1960s. Nowadays, PLA resin is approved by the FDA and European regulatory authorities for use in food delivery systems and drugs.^{9,21} However, although PLLA has some advantages, we find that it also has some disadvantages: as it has high crystallinity and a slow degradation rate, in the body it has an inflammatory effect. Knowing that d-lactic acid has a faster degradation and if L-lactic acid and D,L-lactic acid monomers are used in the preparation of PLLA, the problems mentioned above can be avoided.^{22,23}

The three-dimensional structure of PLA is still a matter of investigation. A series of investigations have been aimed at drawing analogies between lactic acid and aminoacids (*e.g.*, based on the fact that LA can be viewed as an analogue of alanine where the amino group has been replaced by a hydroxyl) – posing the question whether PLA can adopt secondary (and possibly tertiary and quaternary) structural features analogous to those seen in aminoacids. Optimizations of the geometry of the secondary structure of polylactic acid (PLA), consisting of decameric units, analogous to those observed in the structure of proteins – helical

structures (α , π , 3_{10}), as well as a β sheet – were reported using molecular mechanics, methods semiempirical, *ab initio* and density functionals. The best method used (M062x/6-311+G**) predicts that the α , π and 3_{10} structures have very similar energies, with π slightly favored by values within the error limits of the method. Furthermore, a comparison of PLLA with PDLLA revealed that the poly-L lactic acid structure is energetically favored over the PDLLA.²⁴

Calculations were also performed on the chemical shifts for ¹³C NMR, ¹H NMR and infrared (IR) spectra of various possible PLA secondary structures. The calculated spectra did not conclusively allow a correlation with experiment for any single secondary structure type. This was interpreted as either a need to use more appropriate calculation methods, or as evidence that the experimental structure of PLA entails new secondary structure elements, different from those seen in proteins and explored in the computational study.²⁵

Molecular dynamics simulations were also performed, through which the interfacial interaction of polylactic acid with zirconium and hydroxyapatite surfaces was analyzed. In these interactions, the PLA conformations underwent pronounced changes especially when coupling agents were added to bioceramic systems and polylactic acids. Using DFT-optimized polymer interaction energy analyzes and bioceramic surfaces, polylactic acids were observed to bind to polymers in all situations except for the α -helix, which did not attach to the (111) hydroxyapatite surface. Using silane as a coupling agent, it is observed that the interactions between polylactic acids and bioceramic surfaces are more evident.²⁶

The interaction between two polylactic acid chains was also examined. PLLA structures were found to be more stable than poly(DL-lactic acid) (PDLLA) copolymers. By examining the individual structures with HF/3-21G*, the β -sheet dimer was determined to be the most stable and the π -helix dimer was found to be the least stable. As the values obtained were very close, it was difficult to determine which is the most stable geometry.²⁷

It was found that the computational predictions on the relative stabilities are dependent on the methods employed. In the case of PLLA, the α helix is predicted the most stable at empirical and semiempirical methods. The Hartree-Fock methods anticipate the most stable structure is the β -sheet. The DFT methods predict that α , π , 3_{10} helices

have similar energies, in contrast with results obtained with semiempirical and empirical methods. The DFT method with the larger utilized basis set with diffuse function prefigured the most stable of the four structures examined is the π helix and the least stable is the β -sheet. There are the same discrepancies for the PDLA as for the PLLA.

Comparison of protein-like structures with the De Santis experimental structure

The helical conformation of the polylactic acid was analyzed by De Santis and coworkers. They investigated the X ray structure of poly (S lactic acid). The conformation fits a helix characterized by ten monomeric units in three turns and a monomeric repeat on the helical axis equal to 2.78 Å. They related the data to the following bond lengths: O_e-C_α 1.46 Å, $C_\alpha-C_c$ 1.53 Å, C_c-O_e 1.31 Å, C_c-O_c 1.19 Å, $C_\alpha-C_\beta$ 1.52 Å, $C_\alpha-H_\alpha$ 1.05 Å, $C_\beta-H_\beta$ 1.05 Å. The angles were: $O_eC_\alpha C_c$ 109.5°, $C_\alpha C_e O_e$ 110°, $C_c O_e C_\alpha$ 118°, $O_c C_c O_e$ 125°, $O_e C_\alpha H_\alpha$ 109.5°, $O_e C_\alpha C_\beta$ 109.5° and $C_\alpha C_\beta H_\beta$ 109.5°. ^{24,28}

Reported now in Table 1 are the relative energies of the protein-like secondary structures of PLA compared with the structure described by De Santis, all optimized at various levels of theory. The empirical and semiempirical PM6 methods predict the structure De Santis to be the less stable

one. This is not valid in the case of π -L-LA₁₀ (MM method) and β -DL-LA₁₀ (PM6 method) structures. The energy difference towards the most stable structure is 63 kcal/mol in the molecular mechanics and 2 kcal/mol in the PM6 results. The HF methods anticipate the β -L-LA₁₀ sheet the most stable, followed by the De Santis structure. The solvation does not change the relative order of the energies. The relative energy values compared to PDLA are with 10–30 kcal/mol bigger than in the case of PLLA. The density functional methods support the De Santis structure as the most stable. For the M062x/6-31G** method, the relative order of the energies differs between the vacuum and solvated structures. Enlarging from a double-zeta basis set to a triple-zeta basis set with diffuse functions increase the energy differences between the De Santis structure and the other four structures, especially in the case of PDLA. The energy differences between the De Santis structure and the L helices are within 4 kcal/mol at M062x methods. The relative energy compared to β sheet increases to ~20 kcal/mol. Overall, beyond the large differences between the methods listed in Table 1, the highest level of theory so far (M062x functional, parametrized especially for describing non-covalent interactions, and employed here with a triple-zeta basis set and solvation) predicts the De Santis structure to be slightly favored, followed at near-degeneracy by the π helix.

Table 1

The relative energies of the α , π , 3_{10} and β PLA structures; the De Santis structure is arbitrarily taken as reference for each level of theory ($\Delta E(\text{De Santis}) = 0$) (methodology as described in²⁸)

Methods	ΔE (kcal/mol, relative to De Santis)			
	α -L-LA ₁₀	π -L-LA ₁₀	3_{10} -L-LA ₁₀	β -L-LA ₁₀
MM UFF	-62.8	5.4	-58.9	-38.2
PM6-G	-1.6	-0.4	-1.2	-1.1
HF/3-21G*	6.0	11.8	3.7	-1.8
HF/3-21G* water	10.2	11.9	-	-0.6
HF/6-31G*	11.2	9.0	10.7	-3.5
DFT/B3LYP/6-31G*	5.6	2.1	5.0	n.a.
DFT/M062x/6-31G*	-0.2	-3.7	0.8	22.6
DFT/M062x/6-31G**	-0.7	-4.2	0.2	22.2
DFT/M062x/6-31G** water	1.0	0.5	0.5	18.6
DFT/M062x/6-311+G**	3.5	0.8	2.8	20.9

The chain length of the De Santis structure, measured as previously done for the other four structures between the oxygen atoms of the first monomer and the ester oxygen atoms of the ninth monomer (numbering starting from the OH terminus of the polylactide), is presented in Table 2. All methods elongate the helix by 3.5 –

3.8 Å from the initial length of 18.92 Å. The MM and PM6 methods generate De Santis helix length close to π -L-LA₁₀. The HF methods give helix lengths longer by 6.2-10.5 Å than the length of α , π and 3_{10} helices. The helix length calculated with DFT methods are also longer with 10-16 Å.

Table 2

The helix length of the structure described De Santis and α , π , 3_{10} helices (values shown in grey are from reference²⁸)

Methods	Helix length(Å)			
	De Santis	α -L-LA ₁₀	π -L-LA ₁₀	3_{10} -L-LA ₁₀
MM UFF	23.4	12.3	24.0	12.1
PM6-G	25.6	12.7	25.4	14.4
HF/3-21G*	23.1	12.6	16.7	12.7
HF/3-21G* water	23.3	13.8	16.2	n.a.
HF/6-31G*	23.6	13.9	14.2	14.3
DFT/B3LYP/6-31G*	23.7	13.3	14.0	13.9
DFT/M062x/6-31G*	22.4	12.0	12.1	12.1
DFT/M062x/6-31G**	22.4	12.0	12.1	12.0
DFT/M062x/6-31G** water	22.8	12.3	12.6	12.5
DFT/M062x/6-311+G**	22.9	12.1	12.2	11.4

Ramachandran analysis of optimized PLA structures

The above-reported data, as well as all the previous computational reports on putative secondary structure elements in PLA, have described the optimized

geometries in terms of relative energies and of gross parameters such as helix lengths. However, no assessment was given of the extent to which the values of the Φ and ψ angles in the sense defined in Ramachandran diagram for peptides³⁰ (Fig. 1) were conserved after geometry optimization.

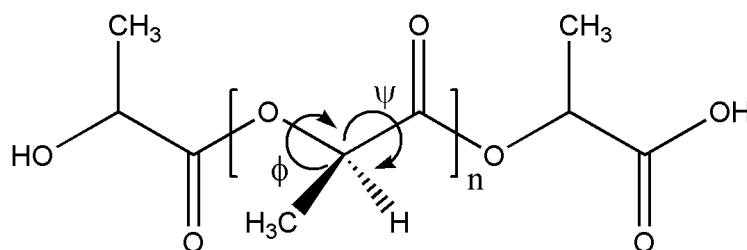


Fig. 1 – Polylactic acid and the dihedral angles of the column Φ and ψ .

The values of the Φ and ψ angles in peptide structures define secondary structure elements as summarized in Table 3. In addition to helices and β sheet secondary structures, another distinct structural motif has been distinguished in which the polypeptide chain reverses direction over the span of only a few amino acids. Such structures are known as ‘turns’. The turns are classified according to the separation between the two end residues: π (the end residues are separated by five peptide bonds $i \rightarrow i+5$), α ($i \rightarrow i+4$), β (i

$\rightarrow i+3$), γ ($i \rightarrow i+2$) and δ ($i \rightarrow i+1$). A β turn is defined for four consecutive residues (denoted by i , $i+1$, $i+2$ and $i+3$) if the distance between the C_α atom of residue i and C_α atom of residue $i+3$ is less than 7 Å and if the central two residues are not helical³⁰. A turn can be converted into its reverse turn by changing the sign on all of its dihedral angles. There are distinct types of β turns (I, I', II, II', III, IV, V, VIa1, VIa2, VIb and VIII) based on the Φ and Ψ dihedral angles of the residues³⁰⁻³³.

Φ and Ψ angles were measured in the optimized geometries of α , π , 3_{10} helices, β sheet and De Santis structure. These values are listed in Table 4 for the M062x data, with graphical representations in Fig. 2. The α , π , and 3_{10} helices all appear to display angles significantly different from the initial values – and all centered around $-60/70$ and $-20/30^\circ$. The similarity among these three optimized structures is mirrored by the similar chain lengths in Table 2, all

suggesting that the three optimized structures essentially describe the same type of secondary structure. The slight energy differences in Table 1 (at the M062x level of theory) are mirrored mainly by slight differences in Φ and Ψ angles at the ends of the decameric chain. The angle values are reasonably similar in all three cases to the type III β turn seen in the canonical Ramachandran peptide classification.

Table 3

Canonical values of Φ , Ψ angles ($^\circ$) for various types of secondary structure

Type	Φ_{i+1}	Ψ_{i+1}	Φ_{i+2}	Ψ_{i+2}
β -Planar sheet	180°	180°	180°	180°
β -Planar sheet	-180°	180°	-180°	180°
β -Pleated sheet	-140°	135°	-140°	135°
α -Helix	-58°	-47°	-58°	-47°
Left-hand α -helix	58°	47°	58°	47°
3_{10} -helix	-49°	-26°	-49°	-26°
π -helix	-57°	70°	-57°	70°
β -Turn				
I	-60	-30	-90	0
I'	60	30	90	0
II	-60	120	80	0
II'	60	-120	-80	0
III	-60	-30	-60	-30
IV	any i to $i+3$ hydrogen bonded turn having angle that differ by more than 40° from those of other β turn types			
VIa1	-60	120	-90	0
VIa2	-120	120	-60	0
VIb	-135	135	-75	160
VIII	-60	-30	-120	120

Table 4

ϕ and Ψ angle values ($^\circ$) of the DFT optimized α helix (initial values are -58° and -47°), π helix (initial values are -57° and -70°), 3_{10} helix (initial values are -49 and -26), β sheet (initial values are 180° and 180°) and De Santis structure (initial values are -29° and 92°)

Starting canonical structure	Optimized ϕ and Ψ				Assignment of optimized structure
	Φ_{i+1}	Ψ_{i+1}	Φ_{i+2}	Ψ_{i+2}	
α helix	-71	-24	-68	-31	β turn III
	-74	-24	-75	-27	
	-73	-29	-71	-29	
	-73	-27	-73	-20	
π helix	-75	-29	-72	-32	β turn III
	-72	-24	-73	-32	
	-69	-29	-72	-31	
	-81	14	-151	43	
3_{10} helix	-71	-23	-68	-30	β turn III
	-75	-25	-74	-25	
	-76	-27	-72	-27	
	-73	-23	-88	-1	
β sheet	-153	-178	-150	-177	δ turn
	-153	-178	-152	-178	
	-152	-176	-149	-177	
	-153	-177	-147	-176	
De Santis	-66	170	-67	172	Not secondary
	-66	170	-66	168	
	-67	171	-66	170	
	-66	167	-69	176	

The δ turn^{33,34} in peptides is defined for 2 residues i , $i+1$, if a hydrogen bond exists between residues i and $i+1$. The weak interactions in the optimized β sheet are between i residue C=O and $i+1$ methyl group. By virtue of this information, it can be said that δ turns may exist in the PLA optimized β sheets. On the other hand, interaction

lengths between i residues C=O and $i+1$ methyl groups exceed the sum of van der Waals radii in the optimized structures described by De Santis. Therefore turns cannot occur in the De Santis structure, nor can one fit the ϕ and Ψ angle values for the optimized structure in any canonical Ramachandran category.

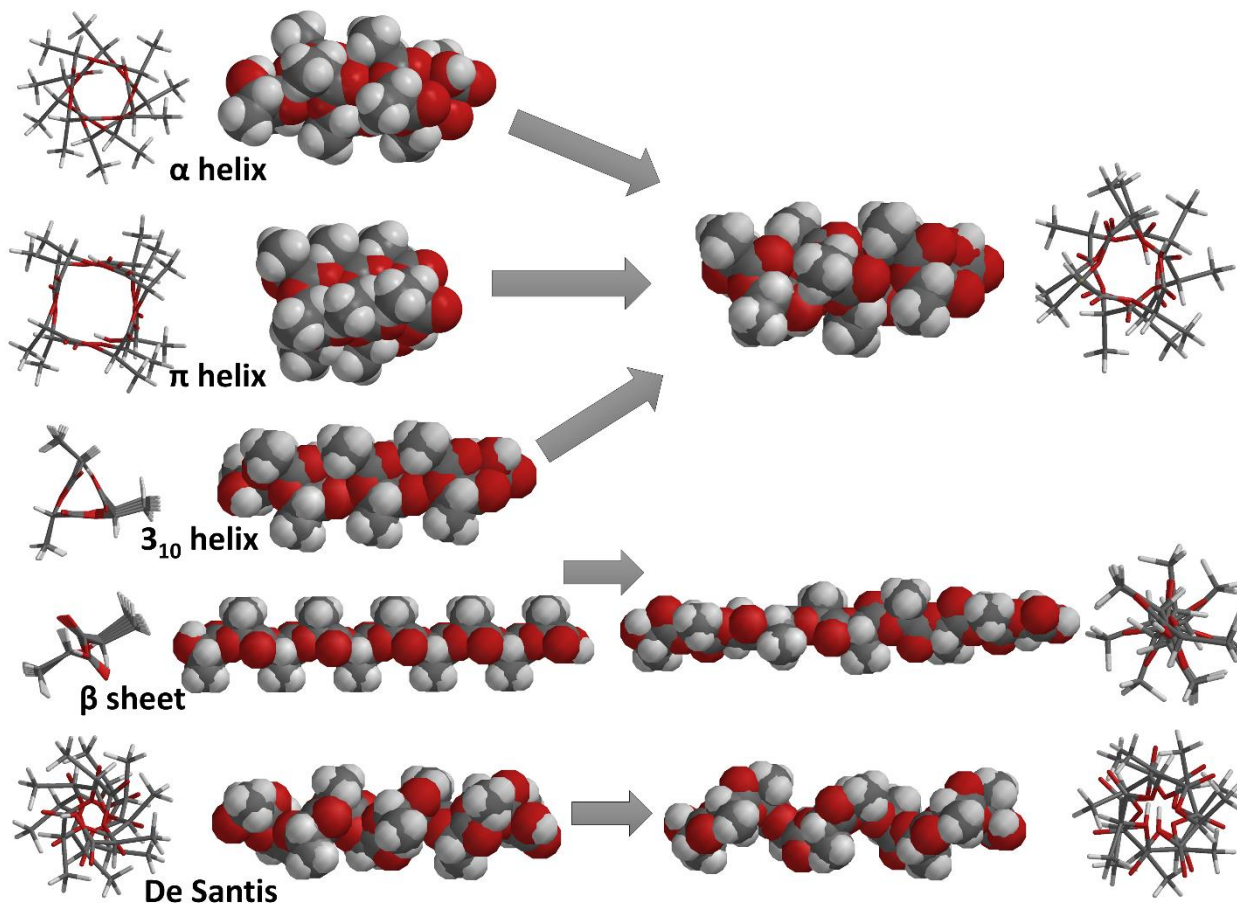


Fig. 2 – Graphical representations of the canonical PLA structures (left) and of the DFT-optimized geometries obtained starting from these structures. See also Table 4 for numerical details.

CONCLUSIONS

The question has been asked, whether in terms of spatial organization for secondary-type structure, polylactic acid (PLA) may be regarded as an analogue of a poly-alanine oligo/polypeptide, where the amino group has been replaced by a hydroxyl. A series of studies have explored the possibility that PLA can adopt peptide-type secondary structures – *i.e.*, repetitive structural patterns characterized by intramolecular hydrogen bonds between neighboring functional groups. To this end, a range of computational techniques have

been applied, looking at relative stabilities of helices (α , π , 3_{10}), and β sheets, as well as at a PLA-specific structure proposed by De Santis. These previous studies have examined the relative energies, general structural features and spectroscopic data of such proposed secondary structure elements of PLA.²⁴ However, while they did note that the computed (geometry-optimized) structures strayed from the initial canonical shape in terms of overall length, they neglected to describe the state of the Φ and Ψ angles after geometry optimization. Reviewing these data with focus on the higher-quality computational method (the M062x functional, parametrized especially for

describing non-covalent interactions – which are the key to describing secondary structure elements), we find that the optimized PLA geometries in fact stray far from the initial Φ , Ψ values – to the extent that all of the peptide-like secondary structures in fact end up as turns (mostly type III β turns – with a δ turn also possible, but disfavored energetically), while the DFT-optimized De Santis structure has no classical correspondent in the Ramachandran series of secondary structures. Thus, within the limits of the computational methods employed so far, only two types of spatial organization are proposed as feasible in PLA: peptide-like type III β turns, and a PLA-specific arrangement (based on the structure proposed by De Santis from experimental data) that has no parallel in classical peptide secondary structures. Unlike in peptide secondary structures, the driving force for repetitive three-dimensional structural organization in PLA is not hydrogen bonding between backbone functional groups, but rather steric repulsions and the weak hydrogen bonding between side-chain CH_3 protons and backbone oxygen atoms.

Supporting information available: Comparative data obtained with other computational methods, comparative data obtained for PDLA.

REFERENCES

1. S. Varadarajan and D. J. Miller, *Biotechnol. Prog.*, **1999**, *15*, 845–854.
2. M. G. Adsul, A. J. Varma and D. V. Gokhale, *Green Chem.*, **2007**, *9*, 58–62.
3. M. Singhvi, D. Joshi, M. Adsul, A. Varma and D. Gokhale, *Green Chem.*, **2010**, *12*, 1106.
4. M. A. Abdel-Rahman, Y. Tashiro, T. Zendo and K. Sonomoto, *RSC Adv.*, **2013**, *3*, 8437.
5. M. A. Abdel-Rahman, Y. Tashiro and K. Sonomoto, *J. Biotechnol.*, **2011**, *156*, 286–301.
6. M. A. Abdel-Rahman and K. Sonomoto, *J. Biotechnol.*, **2016**, *236*, 176–192.
7. O. Martin and L. Avérous, *Polymer*, **2001**, *42*, 6209–6219.
8. R. P. John, G.S. Anisha, K. M. Nampoothiri and A. Pandey, *Biotechnol. Adv.*, **2009**, *27*, 145–152.
9. B. Gupta, N. Revagade and J. Hilborn, *Prog. Polym. Sci.*, **2007**, *32*, 455–482.
10. N. Graupner, A. S. Herrmann and J. Müssig, *Compos. Part. A Appl. Sci. Manuf.*, **2009**, *40*, 810–821.
11. S. Dutkiewicz, D. Grochowska-Ląpienis and W. Tomaszewski, *Fibres Textiles East. Eur.*, **2003**, *11*, 66–70.
12. P. I. Anakhu, C. C. Bolu, A. A. Abioye, G. Onyiagha, H. Boyo, K. Jolayemi and J. Azeta, *Arch. Foundry Eng.*, **2018**, *18*, 65–71.
13. K. Deng, H. Chen, Y. Zhao, Y. Zhou, Y. Wang and Y. Sun, *PLoS One*, 2018, **13**, e0201777.
14. Z. Liu, Y. Wang, B. Wu, C. Cui, Y. Guo and C. Yan, *Int. J. Adv. Manuf. Technol.*, **2019**, *102*, 2877–2889.
15. W. Shao, J. He, Q. Han, F. Sang, Q. Wang, L. Chen, S. Cui and B. Ding, *Mat. Sci. Eng. C*, 2016, **67**, 599–610.
16. W. Gao, Z. Wang, F. Song, Y. Fu, Q. Wu and S. Liu, *Polymers*, **2021**, *13*, 3492. <https://doi.org/10.3390/polym13203492>.
17. G. Li, M. Zhao, F. Xu, B. Yang, X. Li, X. Meng, L. Teng, F. Sun and Y. Li, *Molecules*, **2020**, *25*, 5023.
18. B. M. Chamberlain, M. Cheng, D. R. Moore, T. M. Ovitt, E. B. Lobkovsky and G. W. Coates, *J. Am. Chem. Soc.*, **2001**, *123*, 3229–3238.
19. K. Oksman, M. Skrifvars and J.-F. Selin, *Compos. Sci. Technol.*, **2003**, *63*, 1317–1324.
20. H. Tsuji, *Macromol. Biosci.*, **2005**, *5*, 569–597.
21. J. Nicolas, S. Mura, D. Brambilla, N. Mackiewicz and P. Couvreur, *Chem. Soc. Rev.*, **2013**, *42*, 1147–1235.
22. D. E. Discher and F. Ahmed, *Annu. Rev. Biomed. Eng.*, **2006**, *8*, 323–341.
23. S. Saeidlou, M. A. Huneault, H. Li and C. B. Park, *Prog. Polym. Sci.*, **2012**, *37*, 1657–1677.
24. I. Irsai, C. Majdik, A. Lupan and R. Silaghi-Dumitrescu, *J. Math. Chem.*, **2012**, *50*, 703–733.
25. I. Irsai, A. Lupan, C. Majdik and R. Silaghi-Dumitrescu, *Studia UBB Chemia*, **2017**, *62*, 495–513.
26. I. Irsai, A. M. V. Brânzanic and R. Silaghi-Dumitrescu, *Studia UBB Chemia*, **2021**, *66*, 107–121.
27. I. Irsai, S. Z. Pesek and R. Silaghi-Dumitrescu, *Studia UBB Chemia*, **2022**, *67*, 47–72.
28. P. De Santis and A. J. Kovacs, *Biopolymers*, **1968**, *6*, 299–306.
29. G. N. Ramachandran, C. Ramakrishnan and V. Sasisekharan, *J. Mol. Biol.*, **1963**, *7*, 95–99.
30. P. N. Lewis, F. A. Momany and H. A. Scheraga, *Biochim. Biophys. Acta (BBA) – Protein Struct.*, **1973**, *303*, 211–229.
31. C. M. Venkatachalam, *Biopolymers*, **1968**, *6*, 1425–1436.
32. J. S. Richardson, *Adv. Prot. Chem.*, **1981**, *34*, 167–339.
33. E. G. Hutchinson and J. M. Thornton, *Protein Sci.*, **1994**, *3*, 2207–2216.
34. C. Toniolo and E. Benedetti, *Crit. Rev. Biochem.*, **1980**, *9*, 1–44.

